Strain Estimation of a Steel Specimen Using Digital Image Correlation

Nutan Shukla
Department of Mining Engineering
National Institute of Technology Rourkela
India
nutan.shukla1992@gmail.com

Dr. Manoj Kumar Mishra
Department of Mining Engineering
National Institute of Technology Rourkela
India
mkmishra@nitrkl.ac.in

***Abstract*— In the recent past, Digital Image Correlation as a tool for surface deformation measurement has gained widespread acceptance in various industries. The technique is to find displacements with subpixel accuracy and with simple experimental setup which ensure high accuracy and high efficiency. In this work, the displacement and strain estimation of a dual phase steel undergoing tensile test has been carried out.**
Keywords—Speckle pattern; non-contact based method; Region of Interest; Correlation criteria

I. Introduction

Strain measurement is the key element of material testing in almost any field. Experimental strain analysis has gained popularity in manufacturing industries because of its ability to test the durability and withstand nature of the specimen. Deformation and corresponding strain are vital parameters within engineering and manufacturing projects. However, measuring the parameters outside the laboratory, in real cases, requires a tough choice between conventional methods keeping accuracy, simplicity and cost balanced. The conventional methods are mostly contact based methods which include electrical strain gauges, mechanical dial gauges, acoustic emission techniques etc. But, the contact based methods lack issues like sensitivity to noise, damage to the recording unit, loss of contact of sensors with the surface, influence of environmental noise and temperature, measurement error etc. Non-contact based methods are categorized as interferometric technique and non-interferometric technique which precede contact based methods in terms of accuracy, human error and repeatability of experiment.

Digital Image Correlation (DIC) is a non-contact based optical technique that acquires an image of the object, stores it and performs image correlation analysis to extract full field deformation of that object. It relies on the inherent textures of the measurement surface and do not require the use of structured light sources. The concept involves comparing the gray intensity changes of the object surface in the acquired images with the reference image. In the last few years, the technique has gained popularity and is commonly used as a useful tool for full field deformation measurement in the area of experimental mechanics. The measurement setup required for this technique consists of an imaging device, monocular in case of 2D DIC and stereo for 3D DIC. The schematic layout of a test setup is given in figure 1.

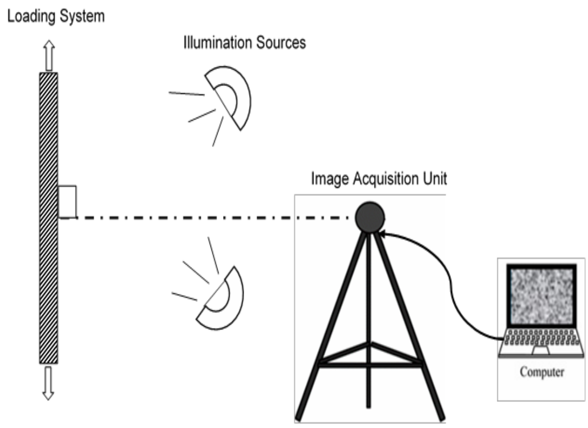

Figure 1: Schematic diagram of DIC setup

The specimen is made to confirm to the ASTM guideline. The operation is carried out in well illuminated environment. The optical axes of the digital camera are set as perpendicular to the measurement surface. Several images are taken during the test and analyzed with respect to the original image i.e. before any loading to get the full field strain contours.

II. Surface Characteristics

The surface pattern plays an important role in measuring the surface strain of the specimen as the analysis is done by comparing the gray intensity changes of the surface. The motion field is computed by comparing point to point matching method between the reference image and deformed image. For this, various subsets are formed to find the correspondence of the pixel of interest in various images [1] [2]. For analyzing the DIC technique, a flat surface is required as textured surface. The random textures also called as speckle pattern are artificially applied on the surface of the specimen before the test is conducted. The speckle pattern and it size is important to ensure accurate and unique identification of the displacements in the deformed image. There are a number of technique available like lithography, stencils, ink, stickers etc. for generating speckle pattern where spray painting is commonly used technique to create speckle pattern [3].

978-1-7281-0174-3/19/$31.00 ©2019 IEEE

A. Spray Paint:

The most common speckle pattern generating technique is with ordinary spray paint. This technique is suitable for any size of specimen where the paint applied on the specimen does not chemically react with the material of the specimen. Generally, the specimen surface is coated with white paint in order to create gradient between the background with the paint [4].

B. Toner:

The toner powder is generally used to generate speckle pattern for very small specimens typically smaller than 12mm. The specimen is coated white and the toner powder is blown with a small lens blower, or by mouth, onto the surface [5].

C. Stencils:

This technique is adopted for very large specimen to achieve perfect speckle pattern. The stencils are made from thin vinyl with water or laser cutting techniques [6].

D. Lithography:

Lithography technique is used for very small sized specimen. Accurate control of pattern location is achievable. This technique is suitable for high temperature and it does not depend on the substrate type. However, this process is time consuming and expensive [7].

E. Ink:

This technique affects surface minimally and high strains can be measured effectively. The ink is dotted on to the surface with a marker to generate speckle pattern [5].

III. OPERATING PRINCIPLE

The fundamental concept of Digital Image Correlation technique involves comparing the deformation of each image of the specimen surface i.e. reference image and set of deformed image. The region of interest (ROI) in the reference image is defined at first while implementing the DIC method. The ROI is further divided into evenly spaced virtual grids or windows to track the changes in each image (Figure 2).

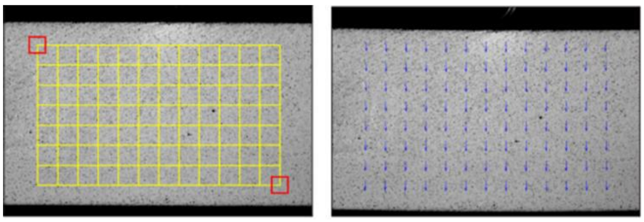

(a) (b)

Figure 2 : (a) Reference image, where red square shows the window used for tracking and the intersection points of the yellow grid are the points to be calculated; (b)The calculated displacement vectors of the deformed image[8].

Each point of the virtual grid is responsible for computation of the displacement to obtain the full-field deformation (Figure 2). The basic principle of 2D DIC is the tracking (or matching) of the same points (or pixels) between the two images recorded before and after deformation (Figure 3). In order to compute the displacements of point P, a square reference subset of (2M + 1) × (2M + 1) pixels centered at point P (x0, y0) from the reference image is chosen and used to track its corresponding location in the deformed image. The square subset matches a wider variation in gray levels which enable specific identification as compared to that in other subsets.

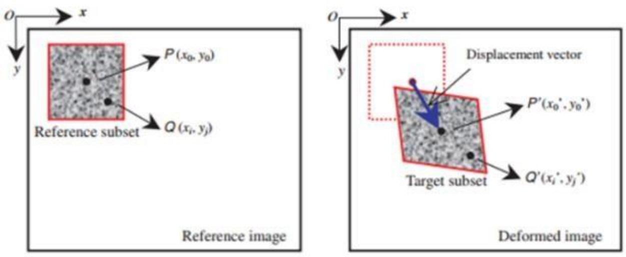

Figure 3: Schematic illustration of a reference square subset before deformation and after deformation [9]

The mapping between the point Q (x_i, y_j) in the reference subset with Q'(xi', yj')in the target subset can be done with a shape function [10] or displacement function [8][11] (Figure 3) and is given by:

$$x_i' = x_j + \xi\left(x_i, y_j\right) \quad (1)$$

$$y_j' = y_j + \eta\left(x_i, y_j\right) \qquad (i,j= -M:M) \quad (2)$$

where the ξ and η identify the analytical formulations of the mapping functions.

Korah et al.[12], proposed polynomial second order shape functions and are by far the most adopted ones and the equations are expressed as:

$$\xi\left(x_i, y_i\right) = u + u_x \Delta x + u_y \Delta y + \frac{1}{2} u_{xx} \Delta x^2 + \frac{1}{2} u_{yy} \Delta y^2 + u_{xy} \Delta x \Delta y \quad (3)$$

$$\eta\left(x_i, y_i\right) = v + v_x \Delta x + v_y \Delta y + \frac{1}{2} v_{xx} \Delta x^2 + \frac{1}{2} v_{yy} \Delta y^2 + v_{xy} \Delta x \Delta y \quad (4)$$

Where, u and v are the x- and y- directional displacement components of the reference subset centre, u_x, u_y, v_x, v_y the first order displacement gradients and u_{xx}, u_{xy}, u_{yy}, v_{xx}, v_{xy} and v_{yy} the second order ones.

IV. CORRELATION CRITERION

Different correlation criterion are used to evaluate the similarity between the reference and deformed subsets for correlation analysis. There exist many definitions of correlation criteria in the literature, that are categorized into two groups, namely CC criteria and SSD correlation criteria [8].

Table 1: Commonly used cross-correlation criterion [8]

CC Correlation criterion	Definition
Cross-correlation (CC)	$C_{CC}=\sum_{i=-M}^{M}\sum_{j=-M}^{M}\left[f(x_i, y_j)g(x_i', y_j')\right]$
Normalized cross-correlation (NCC)	$C_{NCC}=\sum_{i=-M}^{M}\sum_{j=-M}^{M}\left[\frac{\left[f(x_i, y_j)g(x_i', y_j')\right]}{\bar{f}\bar{g}}\right]$
Zero-normalized cross-correlation (ZNCC)	$C_{ZNCC}=\sum_{i=-M}^{M}\sum_{j=-M}^{M}\left\{\frac{\left[f\left(x_i, y_j\right) -f_m\right] \times \left[g\left(x_i', y_j'\right) -g_m\right]}{\Delta f\Delta g}\right\}$

Table 2: Commonly used SSD correlation criterion[8]

SSD Correlation criterion	Definition
Sum of squared difference (SSD)	$C_{SSD}=\sum_{i=-M}^{M}\sum_{j=-M}^{M}\left[f\left(x_i, y_j\right) -g(x_i', y_j')\right]^2$
Normalized sum of squared difference (NSSD)	$C_{NSSD}=\sum_{i=-M}^{M}\sum_{j=-M}^{M}\left[\frac{f\left(x_i, y_j\right)}{\bar{f}} - \frac{g\left(x_i', y_j'\right)}{\bar{g}}\right]^2$
Zero-normalized sum of squared difference (ZNSSD)	$C_{ZNSSD}=\sum_{i=-M}^{M}\sum_{j=-M}^{M}\left[\frac{f\left(x_i, y_j\right) -f_m}{\Delta f} - \frac{g\left(x_i', y_j'\right) -g_m}{\Delta g}\right]^2$

The mean, median and standard deviation are expressed below.

In table 1 and 2,

$$f_m=\frac{1}{(2M+1)^2}\sum_{i=-M}^{M}\sum_{j=-M}^{M} f(x_i, y_j) \quad (5)$$

$$g_m=\frac{1}{(2M+1)^2}\sum_{i=-M}^{M}\sum_{j=-M}^{M} g(x'_i, y_j') \quad (6)$$

$$\bar{f}=\sqrt{\sum_{i=-M}^{M}\sum_{j=-M}^{M}\left[f(x_i, y_j)\right]^2} \quad (7)$$

$$\bar{g}=\sqrt{\sum_{i=-M}^{M}\sum_{j=-M}^{M}\left[g(x_i', y_j')\right]^2} \quad (8)$$

$$\Delta f=\sqrt{\sum_{i=-M}^{M}\sum_{j=-M}^{M}\left[f\left(x_i, y_j\right) -f_m\right]^2} \quad (9)$$

$$\Delta g=\sqrt{\sum_{i=-M}^{M}\sum_{j=-M}^{M}\left[g\left(x_i', y_j'\right) -g_m\right]^2} \quad (10)$$

V. ERROR SOURCES OF 2D DIC

The Digital Image Correlation is one such interferometric technique which can be easily implemented with a simple experimental setup. However, it can also be affected by the measuring system. The accuracy of the DIC system mainly relies on the imaging system, loading system and the selection of the suitable correlation algorithm. The errors related to the imaging and loading system are in selecting the right size of speckle pattern, non-parallel between the acquisition unit and specimen, distortion of images, influence of noise while acquisition and digitization. The errors are also due to inappropriate cross-correlation algorithm and execution are selection of subset size, the cross-correlation criterion, Sub-pixel algorithm, Shape function and Interpolation scheme. The improvement of accuracy of 2D DIC needs estimation of the errors related to different error sources [13]

VI. APPLICATION OF 2D DIC

The Digital image correlation is widely being used in various industries as automobile, civil constructions, ophthalmology, experimental strain analysis etc.

Gali et al. [14] evaluated crack propagation and post-cracking behavior in steel fiber reinforced concrete (SFRC) beams, using full-field displacements obtained from the digital image correlation technique. Surface displacements and strains during the fracture test of notched SFRC beams with 0.5 and 0.75% volume fractions (V_f) of steel fibers were analyzed and established the relation between the crack opening width as a function of crack tip opening displacement and the residual flexural strength of SFRC beams. Lai et al. [15] introduced a method based on digital image correlation (DIC) to measure crack extension in graphite beam specimen, a brittle material. It used DIC with a step function to measure cross-correlation of the displacements. The cross-correlation method successfully identified the path of an advancing crack based on DIC results. Cinar et al. [16] introduced the concept of phase Congruency to detect and quantify cracks and their opening. The accuracy of the proposed algorithm in detecting cracks was compared with conventional method as Heaviside function fitting. It was found that the PC-based method is more accurate and robust to noise than the widely used gradient based and Heaviside algorithms.

The DIC technique was also employed in Ophthalmology. The mechanical properties of retina undergoing tensile loading were observed [17]. It measured the multi-directional corneal strain, thickness and radius of curvature in human eyeballs [18]. The measurement of strain distributions within the articular cartilage and measurement of diabetic retinopathy with the DIC technique were also reported in various literatures [19][20].

The DIC technique was applied to monitor the structural health of man-made structures such as the dynamic displacement of a bridge [21]. It was found that the approach was cheap and simple in comparison to that of Linear Variable Differential Transformers (LVDTs) and dial gauges. In this investigation, DIC approach was used to measure the x-displacement, y-displacement, corresponding strains in x and y directions and the variations of cross-correlation over the deformation on a dual phase steel.

VII. EXPERIMENTATION

The experiment was conducted on a dog-bone shaped dual phase steel of 30 mm and width 5.62 mm. Pastable stickers were used on the surface of the specimen to create speckle pattern. The two ends of the specimen were clamped by the jaw of the Universal testing unit (make: Instron 8862) to experience tensile loading. The image at the beginning was considered as reference image. Loading was applied at a rate of 0.03 mm/sec and continuous images were captured by LaVision Imager E-lite of 1626-pixel × 1236-pixel with an exposure time 100 µs to 80 ms.

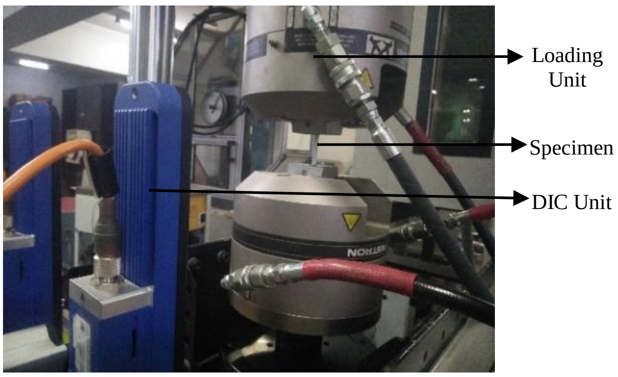

Figure 4: Experimental setup

A total of 769 images were taken from the beginning of the test to end and they were analyzed using LaVision Strain master to calculate the full field displacement. The experimental images of reference image and deformed image are given in figure 5.

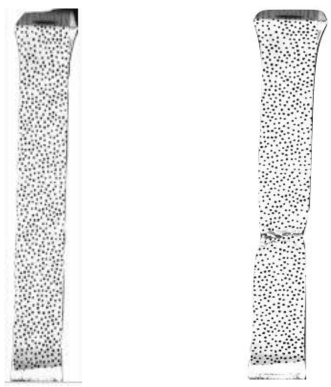

Figure 5: Experimental Images of (a) Reference image and (b) Deformed image

It was observed that the variation of strain from 0 to 100 images were about 3% that increased to 28% at the failure stage. The rate of variation in strain was maximum between 450 to 769 image (Figure 6).

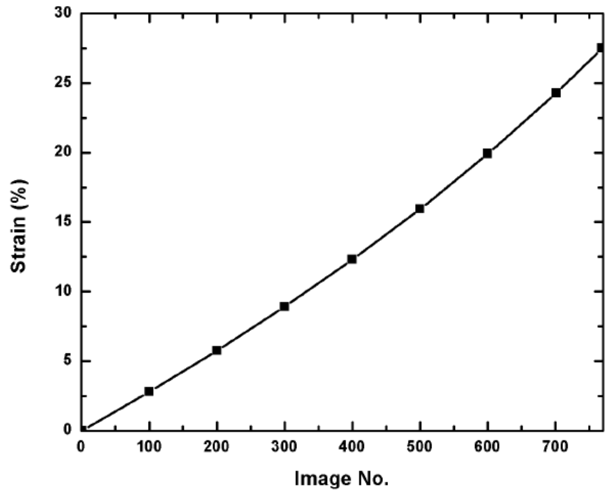

Figure 6: Variation of strain with images

Stress - strain curve is an important element of material testing when it is subjected to loading condition. Here, the strain has been calculated using Digital Image Correlation technique and with the conventional strain gauge for validation purpose. The specimen exhibit strain softening behavior after achieving 3% strain and went on upto 27%. (Figure 7) The elasticity of the specimen was observed upto 400 MPa beyond which the specimen started yielding to load.

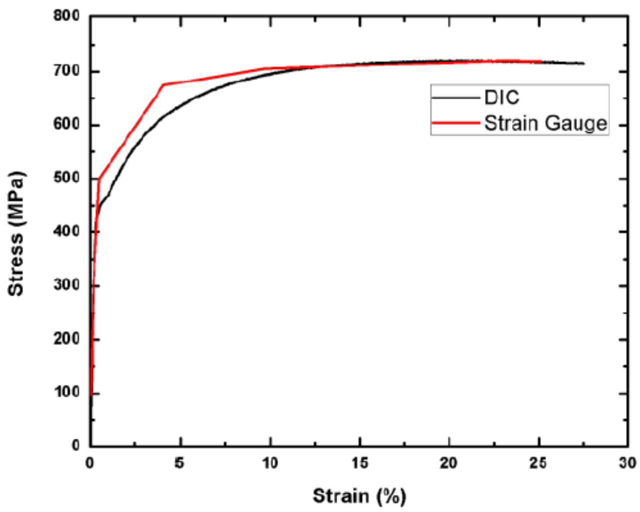

Figure 7: Stress- Strain relationship obtained from DIC and Strain gauge

From the graph, it can be inferred that, upto 570 Mpa the specimen was in elastic zone having a strain of 2.3% which is quite less. But as the stress increased, corresponding strain also increased and failure occurred. The DIC method is well backed up by the conventional strain gauge method with a correlation of 97.6%.

The DIC technique can be a better solution over contact based technique i.e. strain gauge as it is more vulnerable to breakage and environmental noise.

The vertical and horizontal displacement are calculated by finding correlation between the reference subset and deformed subset. The reference image was split into a number of subsets that were further processed in many intermediate stages before obtaining the final position. The vertical elongation was less than that of horizontal elongation obtained during the test. (Figure 8,9).

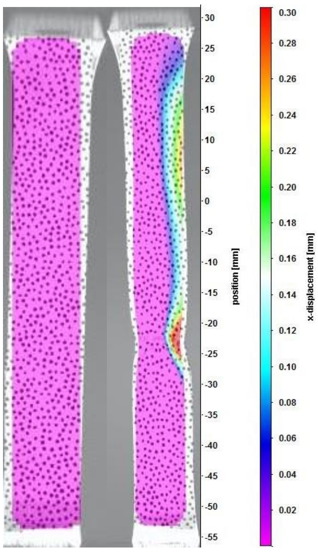

Figure 8: Contour plot of x-displacement of Reference image and Deformed Image

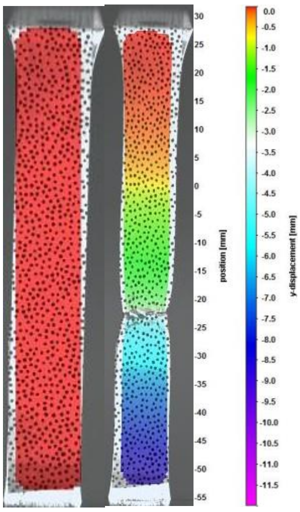

Figure 9: Contour plot of y-displacement of Reference image and Deformed Image

Strain is the ratio of change in dimension to the original dimension. It was observed the vertical strain as 0.275% and the horizontal strain as 1.3%. The vertical strain ϵ_{xx} profile and horizontal strain ϵ_{yy} profile for different loading conditions are given in figure 10, 11.

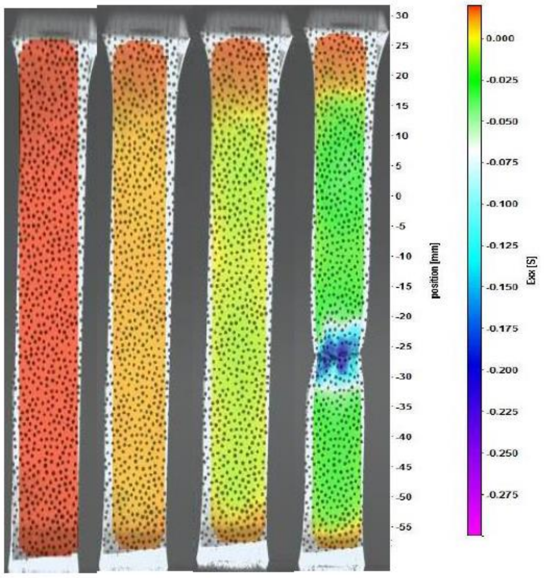

Figure 10: The vertical strain ϵ_{xx} profile at load 0kN, 3.15kN, 3.78kN, 3.93kN

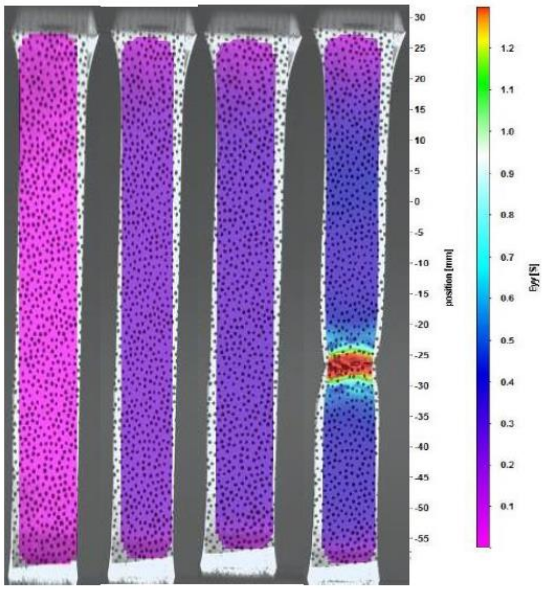

Figure 11: The horizontal strain ϵ_{yy} profile at load 0kN, 3.15kN, 3.78kN, 3.93kN

The strain is calculated by finding correlation between two consecutive images. The reference image has highest correlation coefficient i.e.1 and it gradually decreases to 0.42 with increasing loading. The change in correlation coefficient with the image number is shown in figure 12.

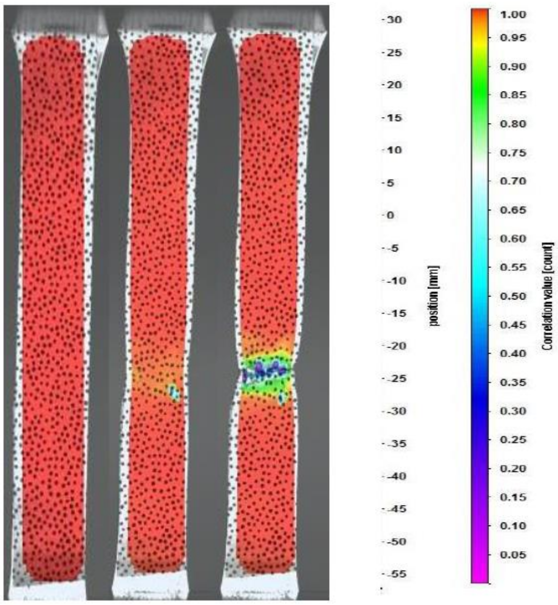

Figure 12: The correlation coefficient profile for Image no.1 (Reference image), 701 (Intermediate image) and 769 (Deformed Image)

VIII. CONCLUSION

There exists no. of techniques for strain estimation like strain gauges, mechanical dial gauges, extensometers etc. which are contact based methods and has lacuna like sensitivity, noise etc. Digital Image Correlation has become widely popular overcoming the issues of contact based methods.

The investigation experimented with a dual phase steel to measure displacements and the corresponding strain values. A total of 769 images were captured and analyzed consecutively. The x and y displacement were calculated and the corresponding strain were analyzed. The stress strain relationship was established. The strain underwent about 28% strain change before failure during the tensile test.

References

[1] Schreier HW, "Investigation of two and three dimensional image correlation techniques with application in experimental mechanics," University of South Carolina, 2003.

[2] J. P. Mellor, "Geometry and texture from thousands of images," Int. J. Comput. Vis., vol. 51, no. 1, pp. 5–35, 2003.

[3] Y. L. Dong and B. Pan, "A Review of Speckle Pattern Fabrication and Assessment for Digital Image Correlation," Exp. Mech., vol. 57, no. 8, pp. 1161–1181, 2017.

[4] Prof. Emanuele ZAPPA, "Novel technique for DIC speckle pattern optimization and generation," 2012.

[5] Z. Chen, C. Quan, F. Zhu, and X. He, "A method to transfer speckle patterns for digital image correlation," Meas. Sci. Technol., vol. 26, no. 9, 2015.

[6] D. Lecompte et al., "Quality assessment of speckle patterns for digital image correlation," Opt. Lasers Eng., vol. 44, no. 11, pp. 1132–1145, 2006.

[7] A. D. Kammers and S. Daly, "Small-scale patterning methods for digital image correlation under scanning electron microscopy," Meas. Sci. Technol., vol. 22, no. 12, 2011.

[8] B. Pan, K. Qian, H. Xie, and A. Asundi, "Two-dimensional digital image correlation for in-plane displacement and strain measurement: A review," Meas. Sci. Technol., vol. 20, no. 6, 2009.

[9] W. J. Gale, K. A. Heasley, A. T. Iannacchione, P. L. Swanson, P. Hatherly, and A. King, "Rock damage characterisation from microseismic monitoring," in The 38th US Symposium on Rock Mechanics (USRMS), 2001, pp. 1313–1320.

[10] V. Frid and K. Vozoff, "Electromagnetic radiation induced by mining rock failure," Int. J. Coal Geol., vol. 64, no. 1–2, pp. 57–65, 2005.

[11] H. W. Schreier, J. R. Braasch, and M. A. Sutton, "Systematic errors in digital image correlation caused by intensity interpolation," Opt. Eng., vol. 39, no. November, p. 2915, 2000.

[12] Weber Hoen, "A correlation-based approach to modeling interferometric radar observations of the Greenland ice sheet," Standford University, 2001.

[13] H. Haddadi and S. Belhabib, "Use of rigid-body motion for the investigation and estimation of the measurement errors related to digital image correlation technique," Opt. Lasers Eng., vol. 46, no. 2, pp. 185–196, 2008.

[14] S. Gali and K. V. L. Subramaniam, "Evaluation of Crack Propagation and Post-cracking Hinge-type Behavior in the Flexural Response of Steel Fiber Reinforced Concrete," Int. J. Concr. Struct. Mater., vol. 11, no. 2, pp. 365–375, 2017.

[15] S. Lai, L. Shi, A. Fok, H. Li, L. Sun, and Z. Zhang, "A New Method to Measure Crack Extension in Nuclear Graphite Based on Digital Image Correlation," Sci. Technol. Nucl. Install., vol. 2017, 2017.

[16] A. F. Cinar et al., "An autonomous surface discontinuity detection and quantification method by digital image correlation and phase congruency," Opt. Lasers Eng., vol. 96, pp. 94–106, 2017.

[17] H. M. Wu W, Peters WH, "Basic mechanical properties of retina in simple elongation," J. Biomech. Eng, vol. 109, no. 1, pp. 65–68, 1987.

[18] J. O. Hjortdal and P. K. Jensen, "In vitro measurement of corneal strain, thickness, and curvature using digital image processing.," Acta Ophthalmol. Scand., vol. 73, no. 1, pp. 5–11, 1995.

[19] C. C. Wang, J. M. Deng, G. A. Ateshian, and C. T. Hung, "An automated approach for direct measurement of two-dimensional strain distributions within articular cartilage under unconfined compression," J. Biomech. Eng., vol. 124, no. 5, p. 557–67., 2002.

[20] R. J. Winder, P. J. Morrow, I. N. McRitchie, J. R. Bailie, and P. M. Hart, "Algorithms for digital image processing in diabetic retinopathy," Comput. Med. Imaging Graph., vol. 33, no. 8, pp. 608–622, 2009.

[21] J. J. Lee and M. Shinozuka, "Real-Time Displacement Measurement of a Flexible Bridge Using Digital Image Processing Techniques," Exp. Mech., vol. 46, no. 1, pp. 105–114, 2006.